



## STRUCTURAL ASPECTS OF ANTIFRICTION PROPERTIES BRASS

**Alexandru CHIRIAC, Gheorghe Florea, Marian NEACSU,  
Ioan SARACIN, Olimpia PANDA**

"Dunărea de Jos" University of Galati  
email: sandu.chiriac@yahoo.com

### ABSTRACT

*a + β' brass types with antifriction properties belong to the category of high-tensile brass, alloys which besides Cu and Zn also contain certain alloying materials introduced in order to obtain some special characteristics. It is known that these elements change the limits of the equilibrium diagram, widening or narrowing the phase existence areas.*

KEYWORDS: antifriction, properties brass

If one part of zinc is replaced by another alloying element, the quantity ratio of the solid solutions  $\alpha$  and  $\beta'$  is changed, although the copper content remains the same; depending on the metal added, it is likely to occur a greater or smaller quantity of solid solution  $\alpha$ .

Thus it was established a zinc equivalence of the most important alloying elements - equivalence factors known as Guillet coefficients, which can be

used to calculate beforehand the structure that the alloy will have (Table 1). This paper aims to analyze the structural aspects of the antifriction brass for manufacturing synchronous rings and mobile cones for Dacia Logan cars (Fig. 1).

The chemical composition of this quality brass contains as alloying elements: aluminum, manganese and silicon (Table 2).

**Table 1.** Equalization coefficients by Guillet [1]

Element	Ni	Mn	Fe	Pb	Sn	Al	Si
t [% Zn]	-1.3	0.5	0.9	1	2	6	10

**Table 2.** The chemical composition of brass parts for the manufacturing of antifriction marks

Chemical composition, %					Maximum of impurities allowed, %	
Cu	Al	Mn	Si	Zn	Pb	Fe
57-60	1.5-2	2-4	0.6-0.9	remaining	<0.35	<0.25

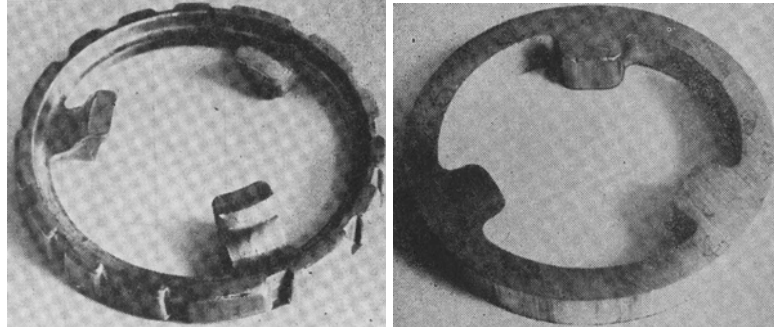
Due to their high equivalence coefficients, aluminum and silicon reduce the amount of the  $\alpha$  alloy phase. Aluminum increases the tensile breaking strength, the yield strength and the hardness of the material, without lowering the values of tenacity; it also improves resistance to corrosion and oxidation. Manganese increases the creeping resistance, the yield strength, the relative elongation and especially the corrosion resistance against sea water. Silicon

increases the tensile strength and the hardness without reducing the plasticity and also improves weldability. As a rough guide, the manufacturing technology of mobile cones includes: alloy elaboration, ingot casting, profiled pipe extrusion and mobile cone stamping (Fig. 1).

The chemical composition of the batches produced in the induction furnaces under charcoal layer varied little from the one presented in Table 3.

**Table 3.** The chemical composition of the batches produced

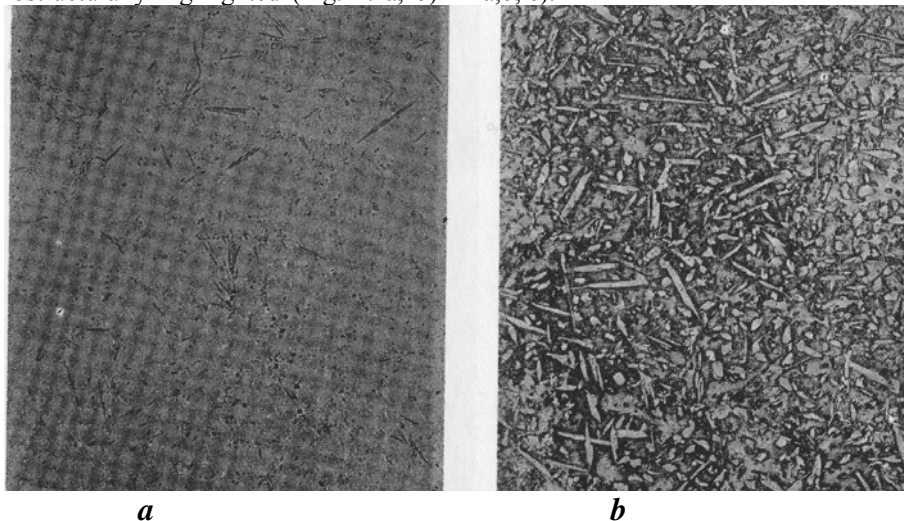
Chemical composition, %					Impurities, %			
Cu	Al	Mn	Si	Zn	Pb	Fe	Sn	P
59.31	1.6	2.58	0.663	remaining	0.035	0.028	0.002	0.006



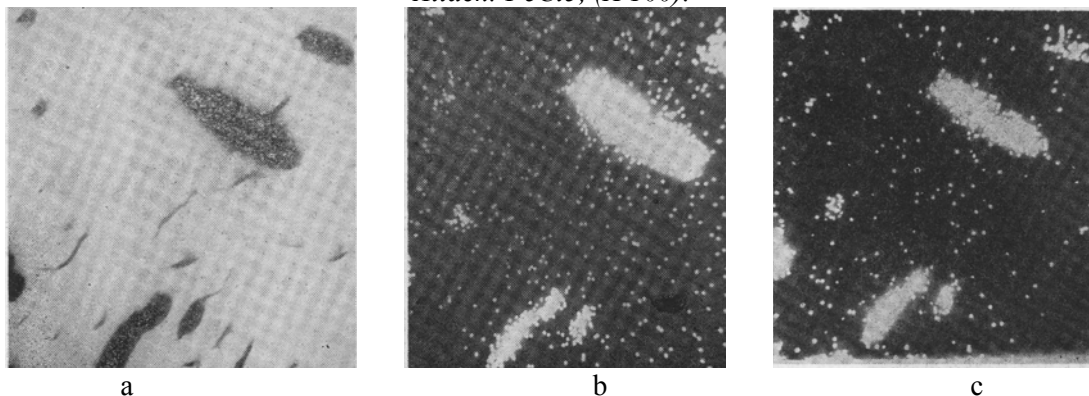
**Fig. 1.** Synchronous rings and mobile cone

The presence of manganese and silicon in the alloy is reflected by the formation of the compound  $Mn_5Si_3$ , macrostructurally highlighted (Fig. 2. a, b)

and confirmed by the analysis of the Mn and Si distribution made with electron microscope (Fig. 3. a,b, c).



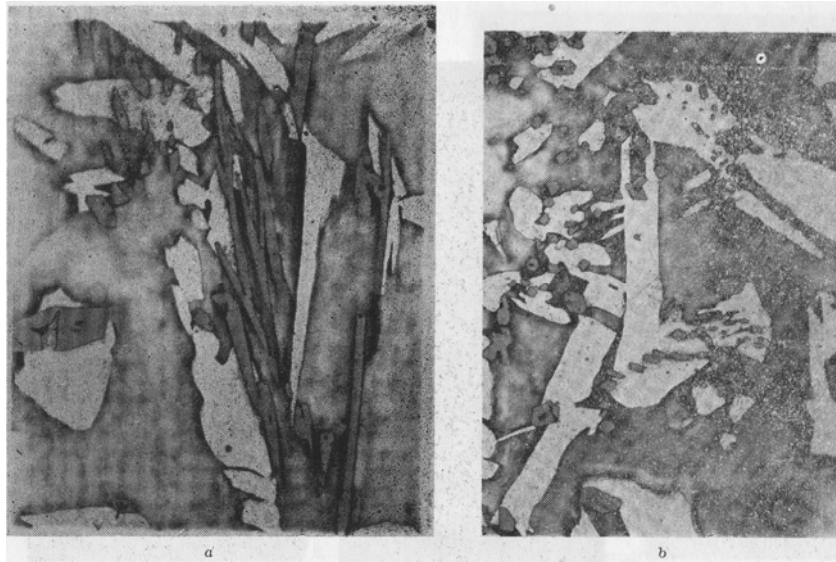
**Fig. 2.** Microstructure of a sample taken from the molten raw material:  
 a –  $Mn_5Si_3$  compound is observed. Open to challenge (X 100); b - mass and solution (dark) is observed solution crystals request a to coloured Light, Attack:  $FeCl_5$ , (X 100).



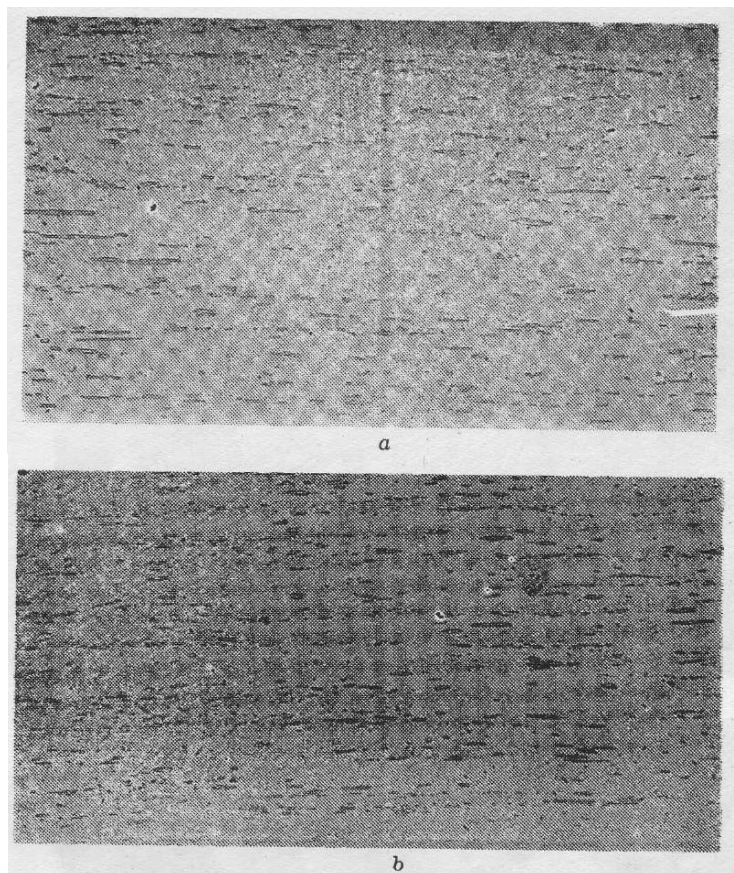
**Fig. 3.** Mn and Si distribution made with electron microscope.

The morphology and distribution of the  $Mn_5Si_3$  compound can be seen in higher magnifications, as shown in Figure 4 a, b. The two phases ( $\alpha + \beta'$ ) have different mechanical properties, phase  $B'$  is hard and

less ductile, while the phase  $\alpha$  is less hard and very ductile. The microhardness of these phases in the molten material are  $HV_{0.01} = 35.4$  for phase  $\beta'$  and  $HV_{0.01} = 29.5$  for phase  $\alpha$ .



**Fig. 4. a, b** Morphology and distribution of the  $Mn_5Si_3$  compound in the cast material. The needle-shaped compound  $Mn Si_3$  (grey) is distributed in the solid solution  $\alpha$  (light colored) as well as in the solid solution ( $\beta'$ ) (dark). Attack;  $FeCl_3$ , ( $\times 1000$ ).



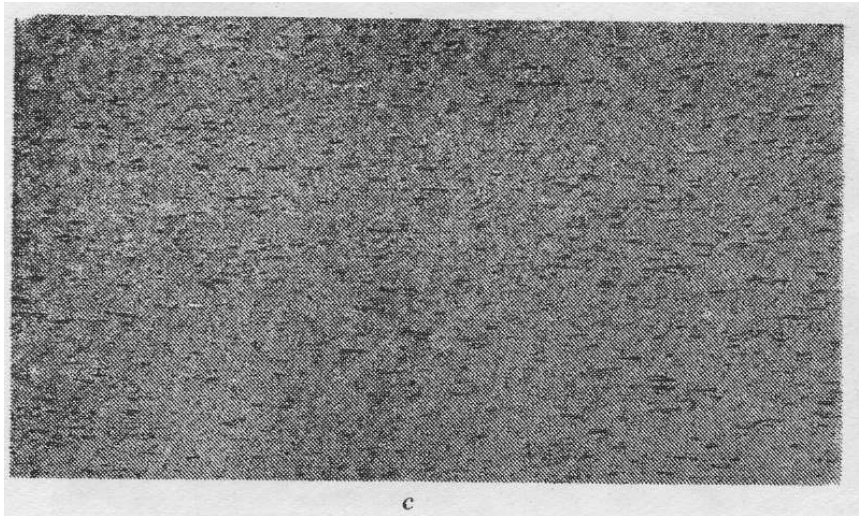


**Fig. 5.** Microstructure of extruded semi-product  
*a*-beginning of extrusion, *b*-middle of extrusion, *c*- end of extrusion.

The mechanical properties of the cast material are presented in Table 4. After extrusion, the  $Mn_5Si_3$  compound structures themselves in rows in the flowing direction of the alloy.

**Table 4.** Mechanical characteristics of the alloy in cast state

No.	$R_{p0.2}$ N/mm <sup>2</sup>	$R_m$ N/mm <sup>2</sup>	$A_5$ %	HB
1	245	476	7.6	156
2	255	476	7.8	156
3	242	490	7.6	157

Because of the metal cooling, during extrusion there is a certain modification in the structure of the material on the workpiece length, as shown in Figures

5. a, b, c and 6. a, b. Table 5 shows the hardness variation along the length of the extruded semi-product.

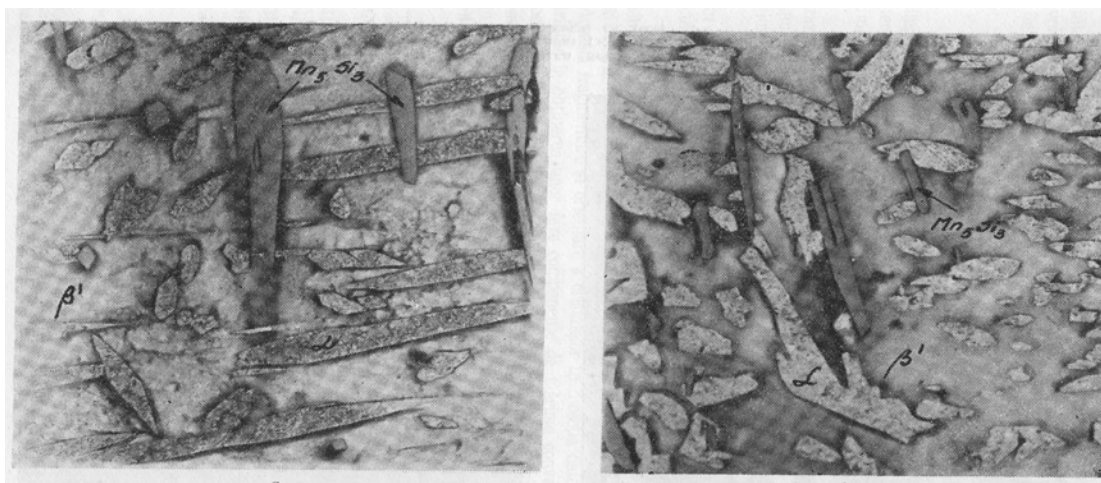


**Fig. 6.** Microstructure of extruded semi-product *a*- beginning of extrusion, *b*- end of extrusion.

**Table 5. Hardness variation along the length of the extruded semi-product**

Distance from the top end of extrusion, mm					
30	400	800	1300	1600	1900
162	170	174	174	176	179
163	174	174	174	178	177
163	175	174	172	177	176

From the data presented in the table it appears that the alloy cooling during extrusion does not strongly influence the mechanical properties of the material. From figures 7 a, b showing the microstructure of the semi-product hot stamping it

appears that the moulding operation does not lead to radical structural changes in the material, the only change being the fragmentation of the Mn<sub>5</sub>Si compound.

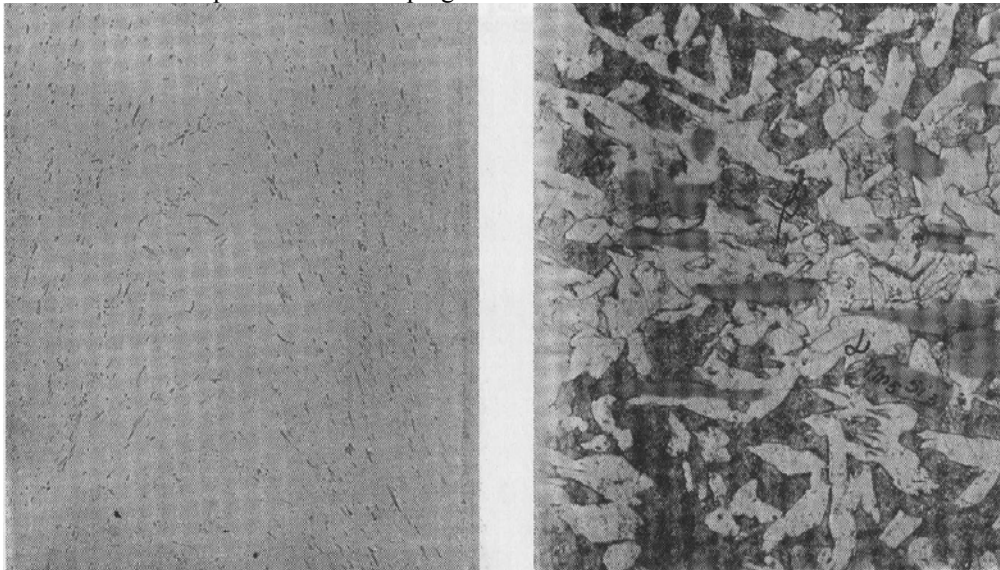


**Fig. 7. a, b. Microstructure of mold semi-product: a - unattacked (x 1000) b-attacked: FeCl<sub>3</sub> (x 1000).**

During plastic deformation (extrusion, stamping), residual internal tensions appear, which are the result of the non-simultaneous volume changes; in order to eliminate these tensions, the mould semi-products were subjected to a tension release treatment at 400-420°C.

### Conclusions

1. The structural analysis of the experimental material has shown the importance of the alloy structure for the imprinting of the mechanical characteristics and of the antifriction properties of the finished product.

Thus, the molten material has specific phases of a biphasic brass ( $\alpha + \beta'$ ) with needle crystallization. This eutectoid structure provides excellent mechanical characteristics but not antifriction properties.

2. From a structural standpoint, the presence of manganese and silicon in the alloy is reflected by the appearance of the needle-shaped compound Mn<sub>5</sub>Si<sub>3</sub> evenly distributed in the mass of material.

3. It is considered that in the case of the studied brass the antifriction properties are ensured by hot plastic deformation. At the extruded and mold material, a fragmentation of all component phases could be noticed. This fragmentation and the crystal orientation in the deformation direction contribute to the obtaining of convenient size phase components, dispersed uniformly throughout the mass, structure which improves the mechanical features and antifriction properties, characteristics which are absolutely necessary in the process of synchronization, wear and friction during mobile cones operation.

### References

- [1]. Schumann, H. - *Metallurgia fizică*. (Physical Metallurgy) București, 1962.
- [2]. Kurt, Dies - *Cupru și aliajele de cupru în tehnică*. (Copper and copper alloys in engineering) Berlin. 1997.
- [3]. Jolobov, V.V., Zverev, G. I. — *Pressovanie metallov*. Moscova, 1991.
- [4]. \* \* \* - *Îndreptar. Kovka i ștampovka țvetniĥ metallov*. Moscova, 1992.